www.czasopisma.pan.pl www.journals.pan.pl

ARCHIVE OF MECHANICAL ENGINEERING

DOI: 10.24425/ame.2022.141516 2022, Vol. 69, No. 3, pp. 455–469

Binayak NAHAK [1], Anil KUMAR [2], Anshul YADAV [2], JerzyWINCZEK [3]

Investigation of deformation behaviour of steel, aluminium and copper alloys during hydro-mechanical drawing

Received 4 November 2021, **Revised** 4 April 2022, **Accepted** 21 April 2022, **Published online** 7 July 2022

Keywords: hydro-mechanical drawing, EN10130, copper C12200, aluminium 8011, deformation

The hydro-mechanical drawing combines conventional deep drawing and sheet hydroforming and is widely used in the automotive industry. In this study, we designed and fabricated an indigenous experimental set-up that is low cost, low weight and portable. This study investigated the deformation of sheet metals into hemispherical cup-shaped parts made of different materials, viz., aluminium 8011 alloys, copper C12200 and steel EN10130 alloys. The initial thickness of sheet metal was 0.4 mm, the most common thickness range used in automotive applications. The deformation behaviour in terms of dome height has been measured by varying the pressure of the fluids. Aluminium 8011 alloy sheets showed a maximum dome height of 11.46 mm at a pressure of 1.47 MPa with no rupture. Steel EN10130 sheets had a maximum dome height of 10.89 mm at a pressure of 9.31 MPa. It was concluded that the behaviours of materials are different in the hydro-mechanical drawing process than in mechanical tests. Copper C12200 sheet showed superior formability with a maximum dome height of 18.91 mm at a pressure of 7.06 MPa than other materials without fracture.

1. Introduction

Hydro-forming is used to shape sheets using a fluid medium as a soft punch in aerospace and automotive industries. Hydro-forming has many advantages over conventional stamping processes: weight reduction, superior part quality, better

✉ Anil Kumar, e-mail: anilk@knit.ac.in, Anshul Yadav, e-mail: anshulyadav.iitk@gmail.com, Jerzy Winczek, e-mail: winczek@imipkm.pcz.czest.pl

[1]Motilal Nehru National Institute of Technology Allahabad, Prayagraj – 211004, India. ORCID: 0000-0001-6654-0905

[2]Kamla Nehru Institute of Technology, Sultanpur – 228118, India. ORCIDs: A.K. 0000-0002-8436-4906, A.Y. 0000-0003-1380-2662

[3]Częstochowa University of Technology, Częstochowa, Poland. ORCID: 0000-0001-7129-0429

strength, and cost-saving [1, 2]. The sheet hydro-mechanical drawing (also called fluid forming) has gotten much interest in the automotive sector because it produces products with a higher surface quality than standard deep drawing. The sheet hydro-mechanical drawing process is also preferred in the manufacturing sector because of its excellent quality, accurate dimension, large drawing ratio, ease of manufacturing the complex products, excellent stiffness and rigidity of the formed parts, suitability for lightweight and thin sheets, and improved surface quality [3–5]. Sheet metals are preferred for the sheet hydro-forming process because of their variation in size and complexity. It is extensively used for producing automobile, aerospace, and electronic and kitchen items [6]. The combination of deep drawing and sheet hydro-forming can be named sheet hydro-mechanical forming. This process provides uniform deformation of sheet metal with a good combination of surface finish and high dimensional accuracy. Nakamura et al. [7–9] proposed hydraulic counter-pressure assisted hydro-mechanical deep drawing in 1984. Automotive applications of sheet hydro-mechanical forming and its development to some extent have been discussed by several researchers [4, 10].

Selection of material and fluid pressure are two major challenges in the sheet hydro-mechanical drawing process. There must be a balance between the ductility of the chosen material and the applied fluid pressure [11]. The material used for sheet hydro-mechanical drawing should have properties such as high ductility, uniform elongation, a large strain hardening coefficient, a fine grain structure [12]. Aluminium, steel, copper and titanium alloys are the preferred materials for lightweight, high strength parts via sheet hydro-mechanical drawing [13–17]. The successful drawing of an aluminium sheet of 0.8 mm thickness was performed with a drawing ratio of 3.3 by supplying a radial pressure of only 25 MPa. Thiruvarudchelvan and Travis [18] reported that hydraulic application of pressure in deep drawing could develop deep cups in a single drawing instead of multiple drawings in the conventional drawing. Kim et al. [19] proposed a new method for hydro-mechanical reverse redrawing assisted by different radial pressure for increasing the drawing ratio up to 4. Janbakhsh et al. [20] performed a numerical simulation of hydro-mechanical deep drawing for Haynes 230 Nickle-based superalloy. Karajibani et al. [21] introduced a simulation-based approach for the determination of the drawing limit of aluminum-1100/copper-C10100 alloys. Yaghoubi and Fereshteh-Saniee [22] studied the hydro-mechanical deep drawing process of bimetallic specimens analytically, experimentally, and numerically. They found that increasing the fluid pressure up to 15 MPa enhanced the quality of the final product.

Although several researchers have studied the deformation behaviour of aluminium, copper and steel alloys through deep drawing and hydro-mechanical drawing, no one has attempted the hydro-mechanical drawing process for aluminium 8011, copper C12200, steel EN10130 alloys. The novelty of the current study is the design and development of an in-house experimental set-up for hydro-mechanical drawing. The indigenous designed experimental set-up was developed with locally available materials with the help of different machines/equipment available in the Institute workshop. The developed experimental set-up is low cost, low weight and portable. The sheet hydro-mechanical forming set-up available in the market are bulky and have a very high cost. The developed set-up is used to form cups of different heights by applying different fluid pressures. The present experiment aims are to analyse and compare the deformation behaviour of aluminium 8011, copper C12200, steel EN10130 sheet metals using a sheet hydro-mechanical drawing set-up to obtain hemispherical cup shape pieces at different fluid pressure. The formability of aluminium 8011, copper C12200, steel EN10130 sheet materials was observed by varying the applied pressure without burst and tears.

2. Experiments and methodology

2.1. Material selection

The aluminium 8011, copper C12200, steel EN10130 material in the form of sheets were purchased from ARK Metal and Alloys, Kanpur, India. The aluminium 8011 alloys were selected because of their excellent surface properties, wettability, and corrosion resistance [23]. The steel EN10130 alloy was selected because of its properties, such as high elongation and good surface finish [24]. The copper C12200 alloy was selected because of its properties, such as excellent ductility [25] and good formability [26]. Square shaped sheets of dimension 80 mm × 80 mm × 0.4 mm were used as the workpiece material. The composition of aluminium alloy 8011, C12200 copper alloy, EN10130 steel alloys are listed in Table 1. The experimental mechanical properties of these materials are included in Table 2.

Table 1. Chemical composition of the selected workpiece [27–29]

Element [%]	Aluminium 8011 alloy	Copper C12200 alloy	Steel EN10130 alloy
Al	Balance	–	–
Cu	–	Balance	–
Fe	0.70	–	Balance
Si	0.60	–	0.05
C	–	–	0.08
Mn	0.10	–	0.4
P	–	0.03	0.04
S	–	–	0.03

Table 2. Mechanical properties of blank materials

Property	Aluminium 8011 alloy	Copper C12200 alloy	EN10130 Steel
Density (kg/m^3)	2700	9000	7800
Elastic Modulus (GPa)	69	120	210
Yield strength (MPa)	95	92	141
% of elongation	22	43	38
Poisson ratio	0.33	0.34	0.30
Tensile strength (MPa)	110	240	293

2.2. Sheet hydro-mechanical drawing process

An in-house developed sheet hydro-mechanical drawing set-up was used for the deformation of the sheets. The experimental set-up consists of various parts, as schematically represented in Figs. 1 and 2. The sheet hydro-mechanical drawing set-up was fabricated along with all required subassemblies, assemblies, essential tools, clamping devices, etc. The items used in the sheet hydro-forming set-up were the electric motor, the vane pump, the hydraulic tank, the cover plate, the relief valve, the filter, the pressure gauge, the hydraulic oil, the die, the coupling, the slots, and the on/off valve. The die and the blank holder with oil sealing are presented in Fig. 3. The die is arranged in the inverted position in the assembly to facilitate the natural drainage of the hydraulic fluid. The die is opened and closed with the help of bolts and nuts, which fasten it properly. Proper positioning and alignment of the die have been taken care of by the drain channel cavity. The workpiece is positioned over the die with the blank holder, and the silicon ring provides sealing of oil in the die holder. The fasteners on the die and the blank holder are sufficiently tightened. The punch is fastened to the hydraulic cylinder's piston

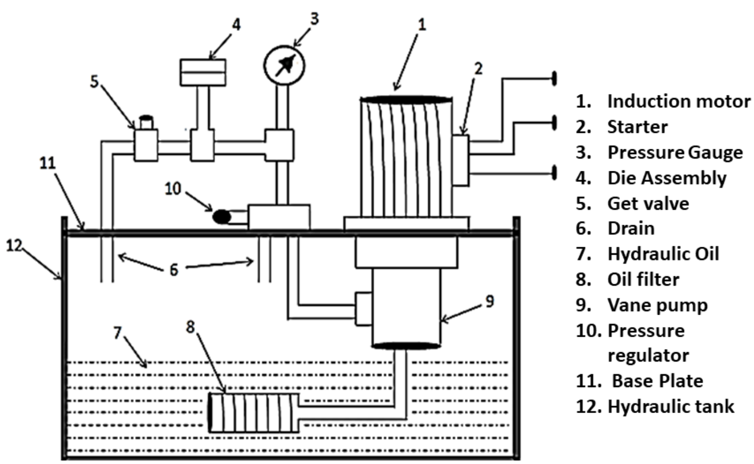

Fig. 1. Schematic of sheet hydro-mechanical drawing set-up

above the cylinder. The cost of cup production with this indigenously developed experimental set-up is approximately 40% of the cost of cup production with other available similar equipment. It shapes the sheet metal by directly applying fluid pressure, which generates a delicate surface. It also helps to control the clamping or easy dissembling of the die. Moreover, it improves the formability with the variation of both pressure and thickness of sheet metal. It is easily repairable. Its maintenance cost is low. There are only minor errors in the deformed part.

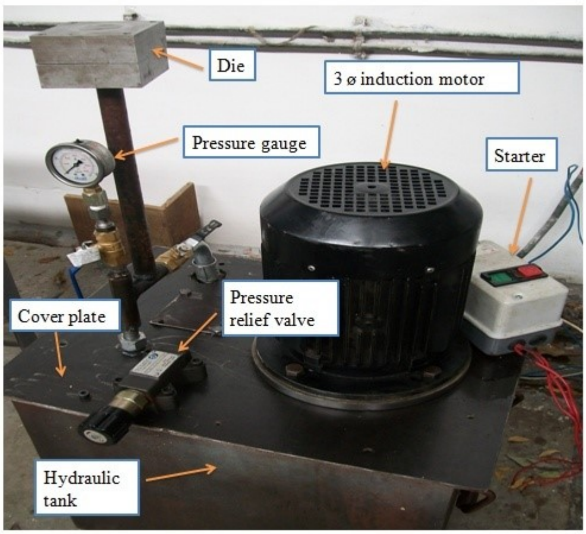

Fig. 2. Sheet hydro-mechanical drawing set-up

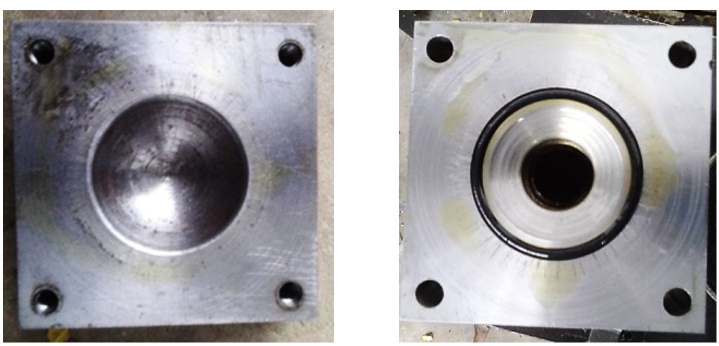

(a) (b)

Fig. 3. Hemispherical die (a) and oil seal attached blank holder (b)

During hydro-forming, a sheet, first of all, bulges out. The forming is performed under pure stretching mode at the pole region and deep drawing mode at the flange region simultaneously. Thinning at the pole due to stretching can be reduced with favourable deep drawing mode in the flange region. This continues till the sheet bulges out to the depth of a die. In the next stage, the drawing of the sheet continues without any stretching at the pole. Finally, corners are formed under the pure stretching mode of deformation, which causes excessive thinning and eventually failure in the corners. Different stages of deformation (bulging, drawing, and forming of corners) during the hydro-mechanical forming of a hemispherical cup process have been recorded.

The workpiece deforms due to the hydraulic pressure, and the pressure gauge records the pressure reading simultaneously. The product is removed after the workpiece is completely deformed. Several sheet hydro-mechanical investigations have been conducted using the sheets under various fluid pressures.

After the experiments, the sheet initially protruded due to hydraulic pressure. During the deformation of the sheet, it was observed that the sheet stretched at the pole region. The sheet also undergoes the deep drawing at the flange zone. This deformation process is carried out until the sheet stretches to the deepness of the die. Further, the sheet drawing is maintained without stretching at the pole region. Lastly, the curved zone of the sheet metal is deformed under stretching conditions, which results in extreme thinning and, ultimately, breakdown occurring at the corner portion. Therefore, various types of deformation, as mentioned in previous section, are observed throughout the hydro-mechanical drawing of a hemispherical cup. The final dome height was measured with a Bosch laser distance measure. The initial and final thickness of the sheet was measured with a wire gauge.

3. Results and discussion

3.1. Hydro-mechanical drawing of aluminium 8011 alloy sheet

Table 3 shows all parameters and the experimental results obtained from sheet hydro-mechanical drawing of aluminium 8011 alloy sheet. The success and failure of each aluminium 8011 alloy sheet sample deformed under pressure is also presented. Fig. 4 shows the variation of the pressure and dome height during the deformation of the aluminium 8011 alloy sheet of 0.4 mm thickness. The hydraulic pressure was varied from 8.82 MPa to 1.37 MPa. The dome height of deformed materials varied non-linearly with the applied fluid pressure. The initial increase in dome height was slightly higher with an increase in fluid pressure, and later due to work hardening a lower effect of fluid pressure was observed in the deformation of the sheet.

Fig. 5 shows the final products obtained after sheet hydro-mechanical experiments corresponding to different hydraulic pressures described in Table 3. The sample deformed at a hydraulic pressure of 8.82 MPa showed a complete fracture because of high hydraulic pressure. The initial fracture was observed in this sample with wrinkles in the flange portion. This primary fracture occurred in the blank material due to a significant variation of hydraulic pressure applied, weak lubrica-

Table 3. Results from sheet hydro-mechanical drawing experiments for aluminium 8011 alloy sheet

Job no.	Pressure [MPa]	Dome height [mm]	Remarks	Reason
1	8.82	23.30	burst	Due to high liquid pressure applied on blank material
2	2.94	15.02	burst	Due to the high thinning ratio at the centre, it bursts from the centre
3	2.45	13.72	burst	Due to the high load rate on blank, it bursts near to pole region
4	1.96	12.98	burst	Due to large pressure and elasticity of the liquid, it bursts at flange area
5	1.86	12.96	burst	Due to variation in the gap between blank material and die, it ruptures
6	1.76	12.87	burst	Due to misalignment of blank with die and blank holder, it bursts from the side
7	1.67	12.65	no burst	Because of good formability and stretching
8	1.47	11.46	burst	The burst occurs due to large strain value which results in stretching of blank material
9	1.37	10.28	no burst	Due to uniform strain distribution, formability of blank material is good

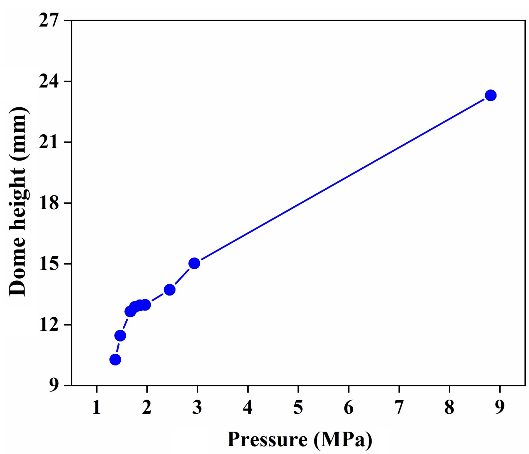

Fig. 4. Effect of hydraulic pressure on the dome height of deformed aluminium 8011 alloy sheet

tion on the sheet flange, minimal gap maintained between the blank holder and the die. Lang et al. [8] reported similar observations during the deep hydrodynamic drawing on an aluminium sheet. There was a little fracture observed in the sample deformed with hydraulic pressure of 2.94 MPa. This fracture was in the curved portion or the wall of the deformed sample. In the literature [30, 31], it was described that in the sheet hydro-mechanical drawing process the loading condition

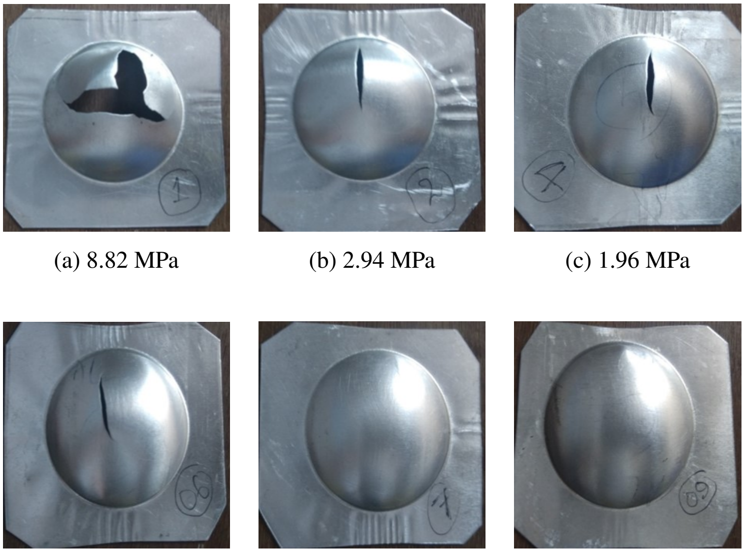

(a) 8.82 MPa (b) 2.94 MPa (c) 1.96 MPa

(d) 1.76 MPa (e) 1.67 MPa (f) 1.37 MPa

Fig. 5. Deformed aluminium 8011 alloy sheet under different hydraulic pressure

depends on the fluid pressure and the blank holding force. The sample failure is dependent on the thinning ratio of the deformed product. The blank holding force is an important parameter for improving the sample thinning because it restrains the material flow. Therefore, the thinning ratio of the sample is one of the significant causes of its fracture. However, the wrinkle occurs in the flange area because the variation of blank holding force generates wrinkles. Primarily, the wrinkle is noticed in the blank material due to the high compressive stress. Furthermore, in the sample deformed at hydraulic pressure of 2.45 MPa we observe the fracture near the hemispherical sample's pole region. This fracture type is noticed as aluminium's drawing limit exceeds the hydraulic pressure. In this figure, the fracture length is small compared to previous samples due to applying low-pressure liquid on blank material. It was interesting to investigate that the fracture length on the sample deformed at 1.96 MPa was greater than in the previous sample, despite the fact that the pressure was smaller. This type of fracture occurs due to the elasticity of the liquid. In addition, the wrinkles observed in this sample are smaller because of the small liquid pressure at the end of the deformation. This may be the non-uniform gap between the blank holder and the die. The sample deformed at a hydraulic pressure of 1.86 MPa showed good deformation with a small fracture at the pole region. Due to the optimized hydraulic pressure, the consistency of drawing of the blank material results in less fracture in the deformed sample. Similarly, the sample deformed at a hydraulic pressure of 1.76 MPa showed more fracture. This fracture occurred because of variation of the gap between the blank material and the die. Similarly, the sample deformed at a hydraulic pressure of 1.47 MPa also shows the fracture due to the same reason. However, the wrinkles were greater in the sample deformed at a hydraulic pressure of 1.86 MPa than in the sample deformed at a hydraulic pressure of 1.76 MPa. The samples deformed at the pressure of 1.67 and 1.37 MPa illustrate the successful deformation, because the improvement of peak pressure enhances deformation in the bottom portion of the blank material, and hence the strains in these regions are also increased. This large strain value results in the stretching of the blank material. However, the uniform strain distribution results in a small thinning at the corner, leading to a better sheet metal formability. Therefore, the thinning in the bottom zone occurs due to the initial bulging [7].

3.2. Hydro-mechanical drawing of copper C12200 alloy sheets

Table 4 shows all parameters and the experimental results obtained from sheet hydro-mechanical drawing of copper C12200 8011 alloy sheet. The success and failure of each copper C12200 8011 alloy sheet sample deformed under pressure is also presented. Fig. 6 shows the variation of the pressure and dome height during the deformation of copper C12200 8011 alloy sheet of 0.4 mm thickness. The hydraulic pressure was varied from 8.82 MPa to 5.88 MPa. The relation between the dome height and the fluid pressure is almost linear. The line slope below the fluid pressure of 7.40 MPa is slightly greater than the slope above 7.40 MPa of fluid pressure.

Table 4. Results from sheet hydro-mechanical drawing experiments for copper C1200 alloy sheet

Job no.	Pressure [MPa]	Dome height [mm]	Remarks	Reason
1	8.82	25	burst	Because of high counter force and pressure at the initial stage
2	7.84	23.60	no burst	Due to high pressure and good wall thickness variation
3	7.35	22.15	no burst	Because of good formability and thinning ratio
4	7.15	18.10	no burst	Due to proper placement of blank
5	7.06	18.91	no burst	Due to low pressure
6	6.86	17.25	no burst	Because of the low load rate
7	6.57	16.79	burst	Because of the low load rate and good thinning ratio
8	6.08	15.45	no burst	Because of the low load rate and a good draw in the bottom portion of the hemispherical part
9	5.88	14.86	burst	Because of large strain on blank material

Fig. 7 shows the final products obtained after sheet hydro-mechanical experiments corresponding to different hydraulic pressures described in Table 4. The samples deformed at hydraulic pressures of 8.82, 6.57 and 5.88 MPa showed the fracture. The burst appeared in the centre region, as depicted in Fig. 7a. This was

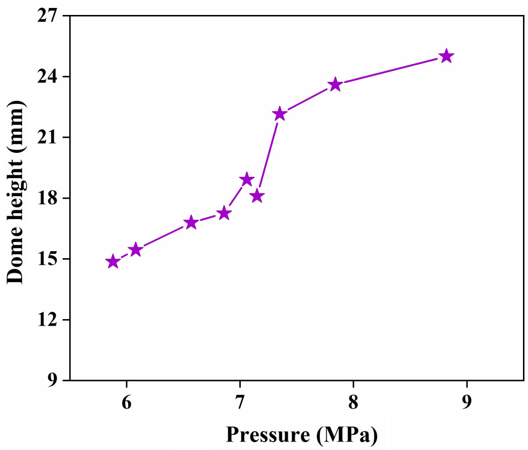

Fig. 6. Effect of hydraulic pressure on the dome height of deformed copper 12200 alloy sheet

(a) 8.82 MPa

(b) 7.35 MPa

(c) 7.06 MPa

(d) 6.86 MPa

(e) 6.57 MPa

(f) 6.08 MPa

Fig. 7. Deformed copper C12200 alloy sheet under different hydraulic pressure

because of the high counterforce and pressure at the initial stage of the drawing process. The counterforce moves the die gradually. On the other hand, a considerable pressure helps to deform the sample rapidly. Hence, a fracture takes place in the centre region. Additionally, the deformed sample contains more wrinkles because high pressure in the die cavity generates heavy wrinkling and buckling of the body. Furthermore, Fig. 7d also shows a fracture in the pole region of the deformed sample due to large strain. Fig. 7f shows the burst at 5.88 MPa. This burst occurred due to pre-bulging and the liquid pressure variation in the primary stage. During the deformation of the copper sheet with the use of higher pressure in the die cavity, the wall thickness significantly varies, following the increase in the measured height. The variation of the blank holding force generates wrinkles. The wrinkle formation reduces as the fluid pressure increases irrespective of material type and thickness variation.

3.3. Hydro-mechanical drawing of steel EN10130 alloy sheets

Table 5 shows the parameters and the experimental results obtained from sheet hydro-mechanical drawing of steel EN10130 alloy sheet. The success and failure of each steel EN10130 alloy sheet sample deformed under pressure is also presented. Fig. 8 shows the variation of the pressure and dome height during the deformation of steel EN10130 alloy sheet of 0.4 mm thickness. The hydraulic pressure was varied from 9.31 MPa to 3.92 MPa. The dome height of the deformed part increases with the pressure applied as the steel has a greater strength and is more rigid compared to aluminium and copper. However, the deformation of steel is more uniform than aluminium and copper, and no burst is observed on the blank.

Table 5. Results from sheet hydro-mechanical drawing experiments for steel EN10130 alloy sheet

Job no.	Pressure [MPa]	Dome height [mm]	Remarks	Reason
1	9.31	10.89	no burst	Because of the high velocity of the fluid and good counter force of die
2	8.82	10.76	no burst	Due to the thinning ratio and proper clamping of blank material
3	8.33	10.25	no burst	Due to good formability
4	7.84	10.08	no burst	Due to low pressure and proper clamping of material
5	7.35	9.47	no burst	Due to the low pressure and low formability of blank material
6	6.86	9.38	no burst	Due to the high internal resistance of blank material
7	5.88	8.67	no burst (auto cut)	Because of the high internal resistance of blank material and die.
8	4.4	6.98	no burst (auto cut)	Because of the high internal resistance of blank material and high strength of sheet metal
9	3.92	6.79	no burst (auto cut)	Because of the high internal resistance of blank material and high strength of sheet metal

Fig. 9 shows the final products obtained after hydro-mechanical experiments on the sheet corresponding to different hydraulic pressures described in Table 5. Fig. 9a depicts the deformed steel blank under the pressure of 9.31 MPa. This deformed sample shows a greater dome height (10.89 mm) due to the high velocity

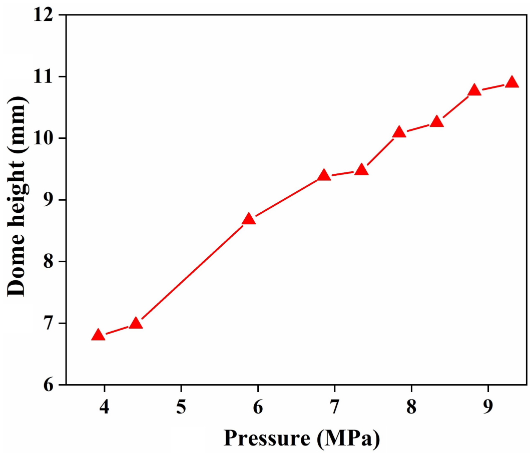

Fig. 8. Effect of hydraulic pressure on the dome height of deformed steel EN10130 alloy sheet

(a) 9.31 MPa

(b) 8.33 MPa

(c) 7.84 MPa

(d) 7.35 MPa

(e) 4.41 MPa

(f) 3.92 MPa

Fig. 9. Deformed steel EN10130 alloy sheet under different hydraulic pressure

of the fluid. On the other hand, Fig. 9f depict a small dome height at the pressure of 3.92 MPa. This occurs because this pressure is insufficient to deform steel which is more brittle and whose strength is high. Fig. 9a shows more wrinkles in the outer edge because of misplacement of the steel blank during hydro-mechanical drawing of the sheet, whereas Fig. 9e depict less wrinkles because of variation of blank holding force. All the samples show no fractures irrespective of the applied pressure. As per the set-up fabrication and die design, the radius of the lower die was 25 mm. However, the steel blanks' dome height was insufficient compared to the die radius. This smaller dome height of the steel blanks indicates that the formability of the blank material is not sufficient. This may be due to insufficient value of the applied fluid pressure. In addition, wall thickness distribution, spring back, dimensional accuracy, etc., of the deformed parts play a vital role during the sheet hydro-mechanical drawing process. The failure like fracture is negligible in all the above-deformed steel blanks, but some samples show wrinkles in the outer region of the blank that appear in the sheet hydro-mechanical drawing process. The experimental results show that the wrinkle formation reduces as the fluid pressure increases irrespective of material type and thickness variation.

4. Conclusions

In this study, the behaviour of aluminium 8011, copper C12200 and steel EN10130 alloys was investigated in the process of deformation into hemispherical cup-shaped parts. An indigenous, low weight, low cost and portable experimental set-up was designed and fabricated. The developed experimental set-up can deform aluminium, copper and steel materials. The height of the cup depends upon the load rate applied in the sheet hydro-mechanical drawing process. As the load rate increased, the height of the cup increased. Similar results can be seen in other materials, but the dome height and burst occurrence depend on the properties of materials. However, the deformation of steel is more uniform than aluminium and copper, and no burst is observed on the blank. Aluminium 8011 alloy sheets showed a maximum dome height of 11.46 mm at a pressure of 1.47 MPa with no rupture. Copper C12200 sheet showed superior formability with a maximum dome height of 18.91 mm at a pressure of 7.06 MPa greater than other materials without fracture. Steel EN10130 sheets had a maximum dome height of 10.89 mm at a pressure of 9.31 MPa. We than conclude that the behaviours of materials in the hydro-mechanical drawing process are different than in mechanical tests.

References

[1] M.-G. Lee, Y.P. Korkolis, and J.H. Kim. Recent developments in hydroforming technology. *Proceedings of the Institution of Mechanical Engineers, Part B: Journal of Engineering Manufacture*, 229(4):572–596, 2015. doi: 10.1177/0954405414548463.

[2] C. Bell, J. Corney, N. Zuelli, and D. Savings. A state of the art review of hydroforming technology. *International Journal of Material Forming*, 13:789–828, 2020. doi: 10.1007/s12289-019-01507-1.

[3] F.T. Feyissa and D.R. Kumar. Enhancement of drawability of cryorolled AA5083 alloy sheets by hydroforming. *Journal of Materials Research and Technology*, 8(1):411–423, 2019. doi: 10.1016/j.jmrt.2018.02.012.

[4] L.H. Lang, Z.R. Wang, D.C. Kang, S.J. Yuan, S.H. Zhang, J. Danckert, and K.B. Nielsen. Hydroforming highlights: sheet hydro-forming and tube hydro-forming. *Journal of Materials Processing Technology*, 151(1-3):165–177, 2004. doi: 10.1016/j.jmatprotec.2004.04.032.

[5] K. Siegert, M. Häussermann, B. Lösch, and R. Rieger. Recent developments in hydroforming technology, *Journal of Materials Processing Technology*, 98(2):251–258, 2000. doi: 10.1016/S0924-0136(99)00206-X.

[6] H. Hu, J.-F. Wang, K.-T. Fan, T.-Y. Chen, and S.-Y. Wang. Development of sheet hydroforming for making an automobile fuel tank. *Proceedings of the Institution of Mechanical Engineers, Part B: Journal of Engineering Manufacture*, 229(4):654–663, 2015. doi: 10.1177/0954405414554666.

[7] T. Nakagawa, K. Nakamura, and H. Amino. Various applications of hydraulic counter-pressure deep drawing. *Journal of Materials Processing Technology*, 71(1):160–167, 1997. doi: 10.1016/S0924-0136(97)00163-5.

[8] H. Amino, K. Nakamura, and T. Nakagawa. Counter-pressure deep drawing and its application in the forming of automobile parts. *Journal of Materials Processing Technology*, 23(3):243–265, 1990. doi: 10.1016/0924-0136(90)90244-O.

[9] K. Nakamura and T. Nakagawa. Sheet metal forming with hydraulic counter pressure in Japan. *CIRP Annals*, 36(1):191–194, 1987. doi: 10.1016/S0007-8506(07)62583-9.

[10] S.H. Zhang, Z.R. Wang, Y. Xu, Z.T. Wang, and L.X. Zhou. Recent developments in sheet hydroforming technology. *Journal of Materials Processing Technology*, 151(1-3):237–241, 2004. doi: 10.1016/j.jmatprotec.2004.04.054.

[11] N. Abedrabbo, M.A. Zampaloni, and F. Pourboghrat. Wrinkling control in aluminum sheet hydroforming. *International Journal of Mechanical Sciences*, 47(3):333–358, 2005. doi: 10.1016/j.ijmecsci.2005.02.003.

[12] M. Koç and O.N. Cora. Introduction and state of the art of hydroforming. In: M. Koç (editor), *Hydroforming for Advanced Manufacturing*, pages 1–29, Elsevier, 2008. doi: 10.1533/9781845694418.1.

[13] M. Chen, X. Xiao, H. Guo, and J. Tong. Deformation behavior, microstructure and mechanical properties of pure copper subjected to tube hydro-forming. *Materials Science and Engineering: A*, 731 (2018) 331–343. doi: 10.1016/j.msea.2018.06.068.

[14] A.A. Emiru, D.K. Sinha, A. Kumar, and A. Yadav. Fabrication and characterization of hybrid aluminium (Al6061) metal matrix composite reinforced with SiC, B_4C and MoS_2 via stir casting. *International Journal of Metalcasting*, 2022. doi: 10.1007/s40962-022-00800-1.

[15] F. Hasan, R. Jaiswal, A. Kumar, and A. Yadav. Effect of TiC and graphite reinforcement on hardness and wear behaviour of copper alloy B-RG10 composites fabricated through powder metallurgy. *JMST Advances*, 4:1–11, 2022. doi: 10.1007/s42791-022-00043-5.

[16] K.S.A. Ali, V. Mohanavel, S.A. Vendan, M. Ravichandran, A. Yadav, M. Gucwa, and J. Winczek. Mechanical and microstructural characterization of friction stir welded SiC and B_4C reinforced aluminium alloy AA6061 metal matrix composites. *Materials*, 14(11):3110, 2021. doi: 10.3390/ma14113110.

[17] L. Prasad, N. Kumar, A. Yadav, A. Kumar, V. Kumar, and J. Winczek. In situ formation of ZrB_2 and its influence on wear and mechanical properties of ADC12 alloy mixed matrix composites. *Materials*, 14(9):2141, 2021. doi: 10.3390/ma14092141.

[18] S. Thiruvarudchelvan and F. Travis. An exploration of the hydraulic-pressure assisted redrawing of cups. *Journal of Materials Processing Technology*, 72(1):117–123, 1997. doi: 10.1016/S0924-0136(97)00138-6.

[19] J.B. Kim, D.W. Lee, D.Y. Yang, and C.S. Park. Investigation into hydro-mechanical reverse redrawing assisted by separate radial pressure—process development and theoretical verification. *Proceedings of the Institution of Mechanical Engineers, Part B: Journal of Engineering Manufacture*, 211(6):451–462, 1997. doi: 10.1243/0954405971516419.

[20] M. Janbakhsh, M. Riahi, and F. Djavanroodi. A practical approach to analysis of hydro-mechanical deep drawing of superalloy sheet metals using finite element method. *International Journal of Advanced Design and Manufacturing Technology*, 6(1):1–7, 2013.

[21] E. Karajibani, R. Hashemi, and M. Sedighi. Forming limit diagram of aluminum-copper two-layer sheets: numerical simulations and experimental verifications. *The International Journal of Advanced Manufacturing Technology*, 90:2713–2722, 2017. doi: 10.1007/s00170-016-9585-1.

[22] S. Yaghoubi and F. Fereshteh-Saniee. An investigation on the effects of the process parameters of hydro-mechanical deep drawing on manufacturing high-quality bimetallic spherical-conical cups. *The International Journal of Advanced Manufacturing Technology*, 110:1805–1818, 2020. doi: 10.1007/s00170-020-05985-5.

[23] Z.P. Xing, S.B. Kang, and H.W. Kim. Softening behavior of 8011 alloy produced by accumulative roll bonding process. *Scripta Materialia*, 45(5):597–604, 2001. doi: 10.1016/S1359-6462(01)01069-7.

[24] A. Hasanbaşoğlu and R. Kaçar. Resistance spot weldability of dissimilar materials (AISI 316L–DIN EN 10130-99 steels). *Materials & Design*, 28(6):1794–1800, 2007. doi: 10.1016/j.matdes.2006.05.013.

[25] B. Meng and M.W. Fu. Size effect on deformation behavior and ductile fracture in microforming of pure copper sheets considering free surface roughening. *Materials & Design*, 83:400–412, 2015. doi: 10.1016/j.matdes.2015.06.067.

[26] A.G. Olabi and A. Alaswad. Experimental and finite element investigation of formability and failures in bi-layered tube hydro-forming. *Advances in Engineering Software*, 42(10):815–820, 2011. doi: 10.1016/j.advengsoft.2011.05.022.

[27] M. Rahimi, P. Fojan, L. Gurevich, and A. Afshari. Aluminium Alloy 8011: Surface characteristics. *Applied Mechanics and Materials*, 719–720:29–37, 2015. doi: 10.4028/www.scientific.net/AMM.719-720.29.

[28] G. Pantazopoulos. Metallurgical observations on fatigue failure of a bent copper tube. *Journal of Failure Analysis and Prevention*, 9:270–274,2009. doi: 10.1007/s11668-009-9225-2.

[29] K.A. Annan, R.C. Nkhoma, and S. Ngomane. Resistance spot welding of a thin 0.7 mm EN10130: DC04 material onto a thicker 2.4 mm 817M40 engineering steel. *Journal of Southern African Institute of Mining and Metallurgy*, 121(10):1–7, 2021. doi: 10.17159/2411-9717/1597/2021.

[30] T. Maki and J. Cheng. Sheet hydroforming and other new potential forming technologies. In: *IOP Conference Series: Materials Science and Engineering*, 418:012117, 2018. doi: 10.1088/1757-899X/418/1/012117.

[31] A.K. Sharma and D.K. Rout. Finite element analysis of sheet hydro-mechanical forming of circular cup. *Journal of Materials Processing Technology*, 209(3):1445–1453, 2009. doi: 10.1016/j.jmatprotec.2008.03.070.